

Classification of Hotspots in Photovoltaic Modules with Deep Learning Methods

Hakan AÇIKGÖZ^{1*}, Deniz KORKMAZ^{2*}, Çiğdem DANDIL³

Electrical and Electronics Engineering, Faculty of Engineering and Natural Sciences, Gaziantep Islamic Science and Technology University, Gaziantep, Turkey

² Electrical and Electronics Engineering, Faculty of Engineering, Malatya Turgut Özal University, Malatya, Turkey

³ Republic of Turkey Ministry of National Education, Fatih Anatolian High School, Hatay/Iskenderun, Turkey

(Geliş/Received: 07/08/2022;

Kabul/Accepted: 07/09/2022)

Abstract: Solar energy systems are increasing their capacity in the energy industry day by day by operating with higher efficiency in parallel with technological developments. The functional operation of photovoltaic (PV) module contributes greatly to the optimal performance of these systems. On the other hand, detection and classification of faults occurring in PV modules are of vital importance in the operation and maintenance of solar energy systems. In this study, the classification of hotspots, which is one of the most common faults in Photovoltaic (PV) modules, is carried out by deep learning methods. First, data augmentation is applied to the images in the training dataset to improve the classification performance. Then, pre-trained deep learning models namely AlexNet, GoogLeNet, ShuffleNet, SqueezeNet, ResNet-50, and MobileNet-v2 are compared on the same test dataset. According to the obtained experimental results, AlexNet has the best performance with an accuracy value of 98.65%, while ResNet-50 provides the worst result with 94.59%.

Key words: Classification, Deep Learning, Hotspot, Photovoltaic Module

Fotovoltaik Modüllerdeki Sıcak Noktaların Derin Öğrenme Yöntemleriyle Sınıflandırılması

Öz: Güneş enerji sistemleri teknolojik gelişmelere paralel olarak daha yüksek verimlilikte çalışarak enerji endüstrisindeki kapasitesini her geçen gün arttırmaktadır. Fotovoltaik (PV) modül hücrelerinin işlevsel bir şekilde çalışması bu sistemlerin en uygun performansı göstermesine büyük katkı sağlamaktadır. Öte yandan, PV modül hücrelerinde meydana gelen arızaların teşhisi ve sınıflandırılması güneş enerji sistemlerinin çalışmasında ve bakımında hayati öneme sahiptir. Bu çalışmada, Fotovoltaik (PV) modül hücrelerindeki en yaygın arızalardan biri olan sıcak noktaların sınıflandırılması derin öğrenme yöntemleriyle gerçekleştirilmiştir. İlk olarak, sınıflandırma performansını arttırmak için eğitim veri setindeki görüntülere veri artırma işlemi uygulanmıştır. AlexNet, GoogLeNet, ShuffleNet, SqueezeNet, ResNet-50 ve MobileNet-v2 gibi ön eğitilmiş derin öğrenme modelleri aynı test veri seti üzerinde karşılaştırılmıştır. Elde edilen deneysel sonuçlara göre AlexNet %98.65'lik bir doğruluk değeri ile en iyi performansa sahipken ResNet-50 ise %94.59 ile en kötü sonucu sağlamıştır.

Anahtar kelimeler: Sınıflandırma, Derin öğrenme, Sıcak nokta, Fotovoltaik modül

1. Introduction

In the last decade, renewable energy sources have started to attract increasing interest, with the consumption of fossil fuels causing severe diseases and environmental pollution [1,2]. Among these renewable energy source types, one of the remarkable clean and reliable energy sources is photovoltaic (PV) based energy systems [3,4]. PV energy systems come to the fore with many advantages such as silent operation, global availability, easy installation, low cost, and pollution-free. However, the PV panels may be influenced by different types of anomalies that impress the credibility and safety of the system operation [5,6]. In addition, Uneven increases in the temperature of their cells, known as PV hotspots, can occur. Hotspot defects appear as highlighted areas in infrared images captured by the thermal Infrared (IR) imaging camera. In hotspot conditions, the affected cells begin to dissipate heat energy instead of generating electrical energy [7,8]. Therefore, early and automated hotspot detection is a crucial defect to provide the reliability of the panels.

Recently, the literature has focused on the detection and classification of hotspots. Le et al. [6] developed a hybrid feature-based support vector machine (SVM) model using infrared thermography technique for hotspots detection and classification of PV panels. They analyzed the PV panels into three different classes as healthy, non-

* Sorumlu yazar: hakan.acikgoz@gibtu.edu.tr. Yazarların ORCID Numarası: ¹0000 -0002-6432-7243, ²0000 -0002-5159-0659, ³0000 -0002-1698-1806

faulty hotspot, and faulty. Their method achieved 92% testing accuracy with low computational complexity structure. Cipriani et al. [9] proposed a convolutional neural network (CNN) model to classify the losses related to PV systems using thermographic non-destructive tests. They achieved an accuracy of 98% in tests that last a couple of minutes. In another study, Ali et al. [7] introduced an early hotspot detection using red-green scale-invariant feature transform descriptor with k-nearest neighbor (KNN) method. In this method, the thermographic is divided into non-overlapping regions and then color image descriptors are calculated for the regions. Their method outperformed all other image descriptors and machine learning combinations with 98.7% accuracy. Dhimish [10] analyzed the machine learning algorithms to early detect PV hotspots. four effective machine learning classifiers as decision tree (DT), SVM, KNN, and discriminant classifiers (DC) were used. The highest detection accuracy was obtained with DC as 98%. Su et al. [11] also proposed a deep learning-based hotspot defect detection method for PV farms. In the model, a residual channel wise attention gate network was designed and distinctive features were extracted. The global average pooling and multilayer perceptron (MLP) were used to dimension reduction of the extracted features. Their method was validated through a real defect detection system and the recall of the hotspot defects reached to 97.06%. Manno et al. [12] introduced a CNN model for use in the effective classification of thermographic images. To decrease image noise, various pre-processing strategies were assessed and they reached an accuracy of 99%. Oliveira et al. [13] presented an aerial infrared thermography analysis for four utility-scale PV plants in the northeast of Brazil. The flight campaign applied different techniques and sensors for each PV power plant. As a result, automated early hotspot defect detection and classification methods have been still studied by designing effective and robust approaches, and also their accuracy performance may still be increased.

This paper presents a comprehensive study on the classification of PV panel hotspot defects using pre-trained deep learning models on infrared thermographic images. These models with two-class classification are applied to define which model reaches a higher hotspot detection accuracy from PV modules. The used dataset is one of the publicly available datasets and it was collected from various large-scale PV farms. In addition, effective offline augmentation methods are utilized to increase and balance the class distribution. In the experimental studies, the metric results are compared and the effectiveness of the deep networks are evaluated. The rest of the paper is presented as: Section 2 describes the classification approach and collected the dataset. In Section 3, the general structures of pre-trained deep learning models are given in detail. Section 4 presents experimental studies and results. Finally, the results obtained from experimental studies are evaluated in Section 5.

2. Classification Approach and Dataset

The scheme of the developed method for the classification of hotspot faults in PV modules is shown in Figure 1. As can be seen in Figure 1, the hotspot and No-Anomaly images are obtained and data augmentation is performed. The obtained dataset is divided into training, validation, and testing dataset. Comparison studies are realized using the most widely used pre-trained deep learning models and metric results are obtained.

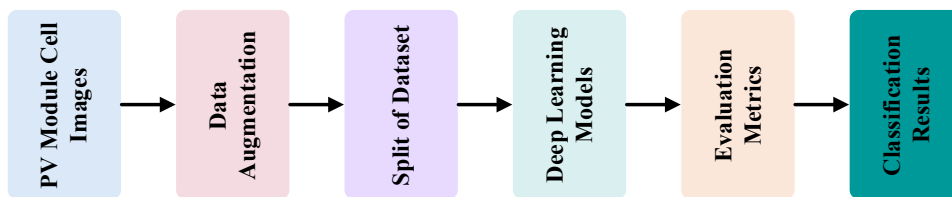


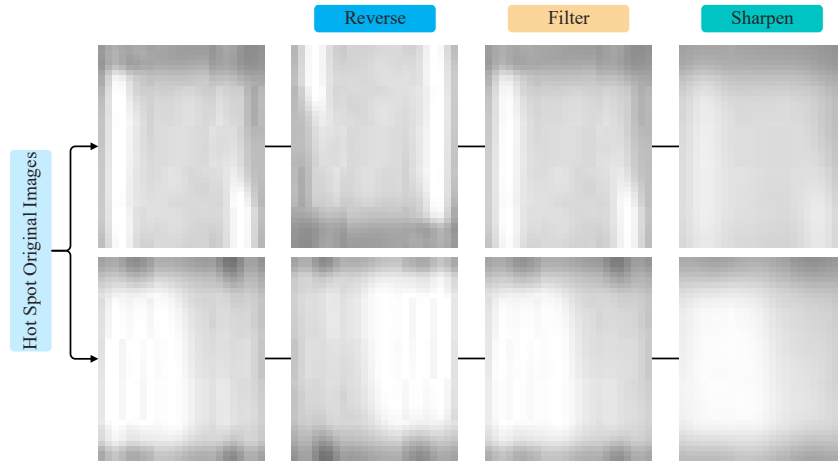
Figure 1. Overview of classification approach used in this study

A publicly available dataset is used in this study [14]. The dataset is obtained from the Raptor Maps Inc team using infrared camera modules [14]. The dataset contains a total of 10,495 images representing 495 hotspot class and 10,000 No-Anomaly class. The each of image in the dataset has 24x40 pixels. The general information about the classes in the dataset is presented in Table 1. As can be seen from Table 1, there is an imbalance in the dataset, which is directly related to the classification performance. The data augmentation is made to deal with this imbalance problem [14].

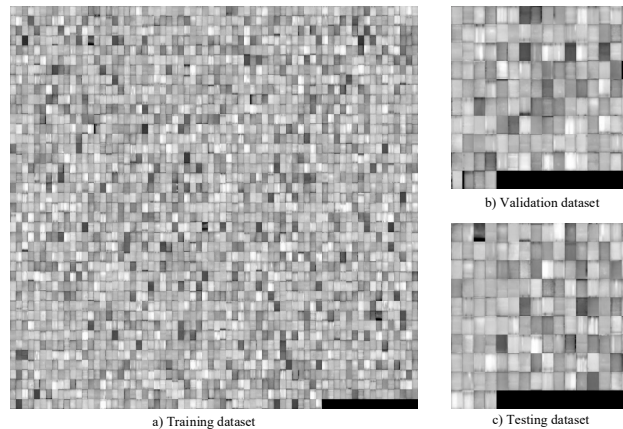
Table 1. Description of classes in dataset

Class	Number of images	Description
Hotspot	495	Hotspot and multiple hotspots on a thin-film modules
No-Anomaly	10,000	Functional solar module
Total	10,495	Total number of images

First of all, 70% of the hotspot images are divided to training, and the rest equally to validation and testing dataset. The reversing, filtering and sharpening processes are applied to images in the hotspot class. After data augmentation process, a total of 1041 synthetic hotspot images are obtained. The sample images of the data augmentation process are shown in Figure 2. Furthermore, 1388 images are obtained for the hotspot class. In the reversing, the hotspot images are rotated 180° counter clockwise. In the filtering process, two-dimensional Gaussian filtering is used. In sharpening process, a Gaussian low-pass filter with a standard deviation of 1.5 is determined.

**Figure 2.** The sample images obtained from data augmentation

In order to eliminate the imbalance in the dataset, the number of images in the No-Anomaly class is equalized to the number of images in the Hot-Spot class, providing a total of 2776 images for the training dataset. In Figure 3, the samples of the dataset divided into training, validation, and testing are presented.

**Figure 3.** The images of training, validation, and testing in the dataset

3. Deep Learning Models

The deep learning models are widely used in many image processing problems. In this study, deep learning models commonly used in the literature such as AlexNet [15], ShuffleNet [16], SqueezeNet [17], ResNet-50 [18], GoogLeNet [19], and MobileNet-v2 [20] are selected. In this section, the brief information about the general features of pre-trained deep learning models is presented. The structures of the pre-trained deep models used in this study are presented in detail in Figures 4-9.

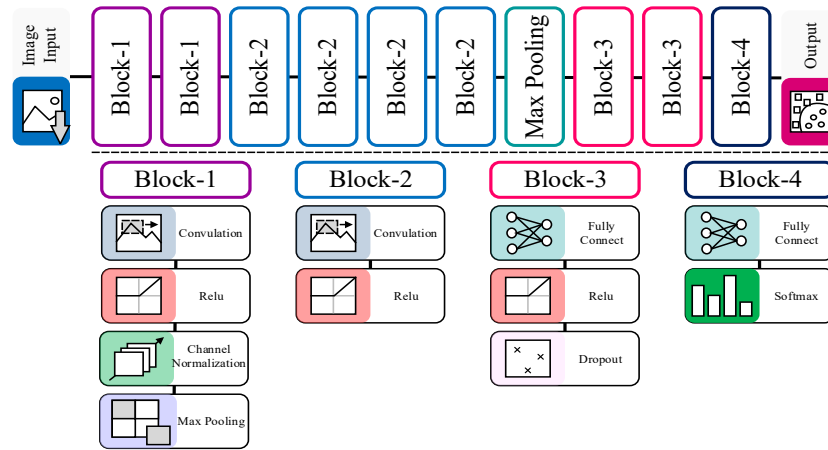


Figure 4. The general structure of AlexNet

AlexNet was proposed by Alex Krizhevsky [15] in 2012 and has features such as superior generalization ability, fast training time and high stability. AlexNet basically includes five convolution layers and three fully connected layers. The input of the AlexNet is $227 \times 227 \times 3$ with RGB depth and the size of each input image is resized according to the input of the network. The convolutions in AlexNet have filters of 96 kernels of size 11×11 , 48 kernels of size 5×5 , 384 kernels of size 3×3 , 384 kernels of size 3×3 , and 256 kernels of size 3×3 , respectively. While the first two fully-connected layers have 4096 neurons, the last one has 1000 neurons. AlexNet performs 3×3 max-pooling with a stride of 2 after convolution-1, convolution-2, and convolution-5.

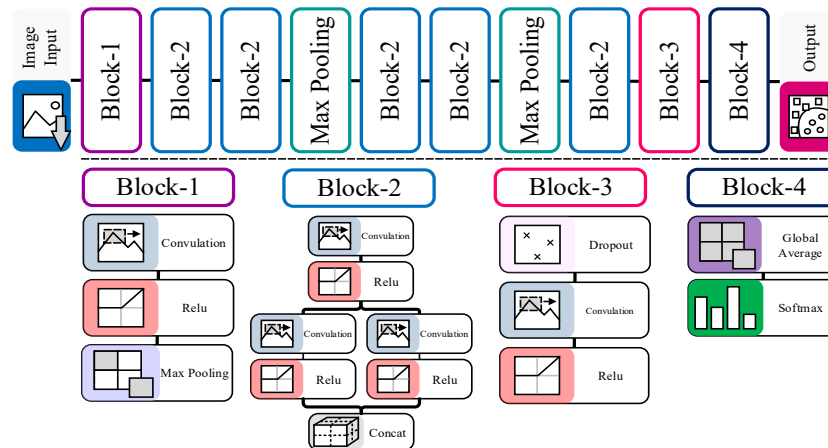


Figure 5. The general structure of SqueezeNet

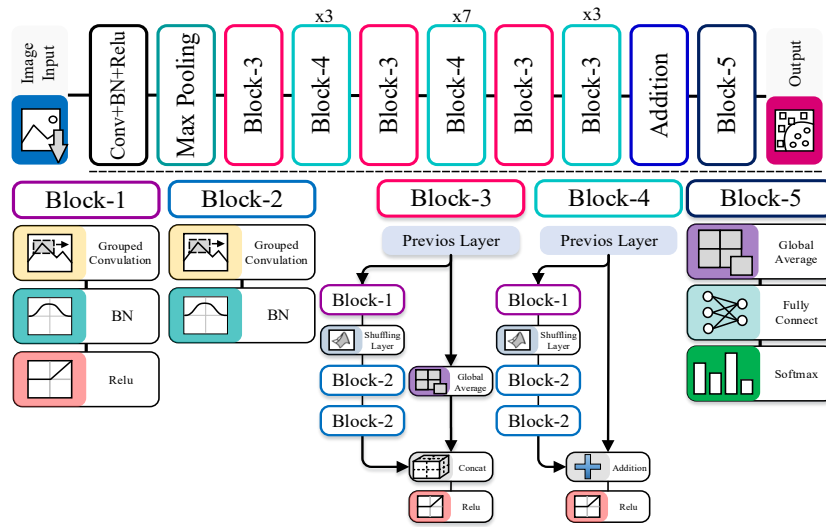


Figure 7. The general structure of ShuffleNet

ShuffleNet was developed for the use of mobile devices with very limited computing power [18]. ShuffleNet performs two operations such as pointwise group convolution and channel shuffle simultaneously to decrease the network computation cost. Through the channel shuffle process used in the network, more durable structures can be obtained with many convolution layers. The input image size of the ShuffleNet is 224×224 and it has fifty layers. The filter sizes of the grouped convolutions in the structure of the network are set as 1×1 , 3×3 , and 1×1 , respectively. The 3×3 average pooling with stride 2 is added in parallel to some units of the network.

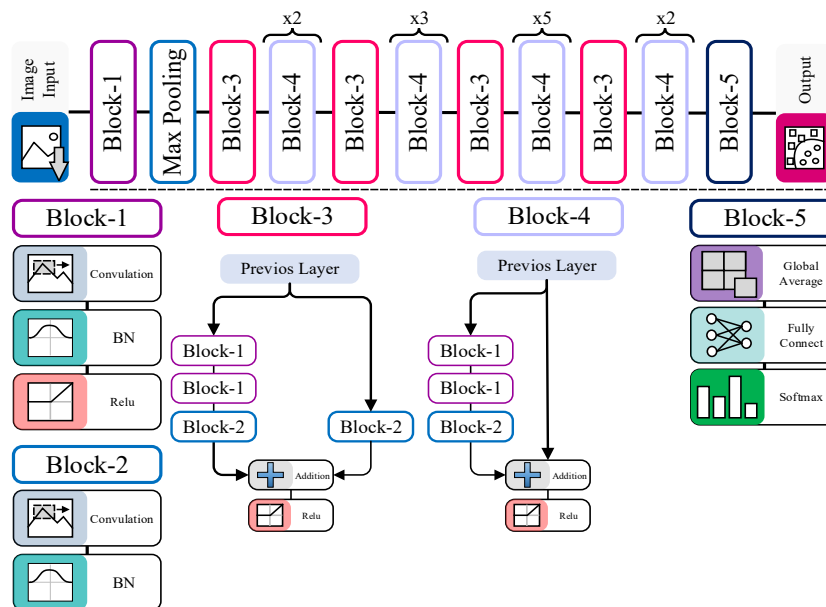


Figure 8. The general structure of ResNet-50

It is known that ResNet-50 has fifty layers [19]. The input image size of the ResNet-50 is 224×224 . The batch normalization layer is used after each convolution and before relu activation. There is a convolution with a kernel size of 7×7 with a stride of 2 at the input of the network. After adding batch normalization and relu to this convolution, the maximum pooling layer with a stride size of 2 is connected. The 1×1 , 3×3 and 1×1 filters are used in convolutions in a building blocks. An average pooling, a fully connected layer and a softmax function are used at the end of the network.

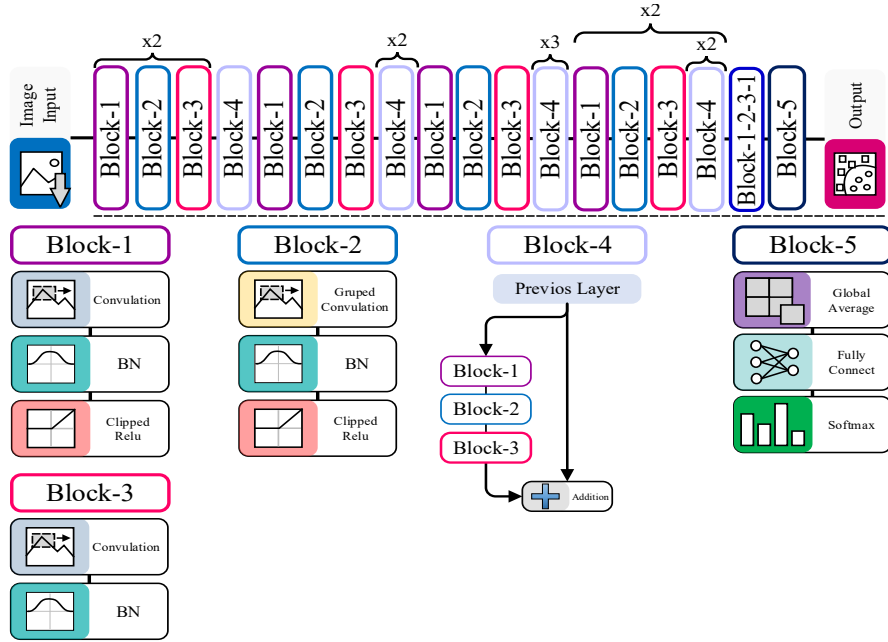


Figure 9. The general structure of MobileNet-v2

MobileNet-v2 is known as a new network developed for mobile and resource-constrained environments [20]. The network is designed to have a new module through the inverted residual with linear bottleneck. This module provides the network with a low-dimensional compressed representation feature that is expanded to high-dimensionality and filtered with a slight depth-based convolution. The input of the network is $224 \times 224 \times 3$ with RGB depth. While the 3×3 filter sizes are used in grouped convolutions in the network, the 1×1 filter sizes are used in others. MobileNet-v2 has only one global average pooling. Some parameters of the deep learning models used in this study are compared in Table 2. As can be seen from the Table 2, while AlexNet has the most parameters among models, SqueezeNet has about 50 times fewer parameters.

Table 2. Comparison of pre-trained deep learning models

Models	Input Size	No. of Layers	Parameters
ResNet-50	224x224	50	25.6M
SqueezeNet	227x227	18	1.24M
GoogLeNet	224x224	22	7M
ShuffleNet	224x224	50	1.4M
MobileNet-v2	224x224	53	3.5M
AlexNet	227x227	8	61M

AlexNet is the first main deep learning model to use GPUs for training. Since AlexNet has less depth, it needs more computation time to learn the features of the images in the dataset. ShuffleNet has less computational cost and comparatively better performance. Although GoogLeNet has relatively few parameters thanks to inception modules, it may not guarantee satisfactory results. Among the deep learning models used in this study, SqueezeNet has the least parameter. MobileNet-V2 with about 3.5M parameters can be considered as a lightweight network which has the deep separable convolution, which increases the computation cost. ResNet-50, which has relatively more parameters, uses residual blocks for better results.

4. Experimental Studies and Results

In this section, the experimental comparison studies are carried out for the classification of hotspots in photovoltaic modules. In these studies, AlexNet, ShuffleNet, SqueezeNet, ResNet-50, GoogLeNet, and

MobileNet-v2, which are commonly used pre-trained deep learning models, are preferred. The same training, validation, and test datasets are applied to each deep learning model. All of our models and studies are carried out on a computer with an Intel (R) i7-10750H CPU @2.60 GHz, NVIDIA Quadro P620 GPU, and 16 GB RAM. Experimental studies are carried out with the help of the R2022a version of Matlab. The stochastic gradient descent with momentum (SGDM) optimizer is used for error minimization with a learning rate of 1e-3. All pre-trained deep learning models are trained for 40 epochs. During training, MiniBatch size is selected as 32.

In order to statistically evaluate the obtained classification results, some performance metric values such as Accuracy, Precision, Sensitivity, Specificity, and F1-score are calculated. These metric values can be expressed mathematically as follows.

$$\text{Accuracy} = \frac{TP+TN}{TP+TN+FP+FN} \quad (1)$$

$$\text{Precision} = \frac{TP}{TP+FP} \quad (2)$$

$$\text{Sensitivity} = \frac{TP}{TP+FN} \quad (3)$$

$$\text{Specificity} = \frac{TN}{TN+FP} \quad (4)$$

$$\text{F1_score} = 2 * \frac{\text{Sensitivity} * \text{Precision}}{\text{Sensitivity} + \text{Precision}} \quad (5)$$

In the equations, expressions such as True Positive, True Negative, False Positive, and False Negative are symbolized as TP, TN, FP, and FN, respectively. Where, TP and TN represent numbers that are actually positive and actually negative, and are correctly predicted, respectively. FP and FN show the numbers that are actually in the negative and positive classes, and that is incorrectly predicted, respectively.

The main target of this study is effectively the classification of hotspots in PV modules. For this purpose, the comparison studies are carried out by deep learning models. First, all deep learning models are trained with the same training dataset and then tested. From these results, the confusion matrix is obtained. The confusion matrices of all deep learning models are presented in Figure 10. As can be clearly seen from Figure 10, AlexNet misclassifies only two images while MobileNet-v2, and ShuffleNet, GoogLeNet, SqueezeNet, and ResNet-50 misclassify 4, 4, 6, 7 and 8 images, respectively.

	AlexNet		MobileNet-v2		ShuffleNet	
Hot Spot	97.4% 74	0.0% 0	98.6% 71	3.9% 3	96.1% 73	1.4% 1
No-Anomaly	2.6% 2	100.0% 72	1.4% 1	96.1% 73	3.9% 3	98.6% 71
	Hot Spot	No-Anomaly	Hot Spot	No-Anomaly	Hot Spot	No-Anomaly
	GoogLeNet		SqueezeNet		ResNet-50	
Hot Spot	95.9% 71	4.1% 3	93.5% 72	2.8% 2	94.6% 70	5.4% 4
No-Anomaly	4.1% 3	95.9% 71	6.5% 5	97.2% 69	5.4% 4	94.6% 70
	Hot Spot	No-Anomaly	Hot Spot	No-Anomaly	Hot Spot	No-Anomaly

Figure 10. The confusion matrices

To highlight the classification performance of deep learning models, statistical evaluation metrics are calculated. The obtained results are listed in Table 3. Moreover, the bar graphs are presented in Figure 11 to better analyze the results in table 3. When the metric results in Table 3 are analyzed in terms of accuracy values, AlexNet provides the best result with 0.9865 among all deep learning models, while ResNet-50 gives the worst result with 0.9459. The accuracy values of SqueezeNet, GoogLeNet, ShuffleNet, and MobileNet-v2 are calculated as being 0.9527, 0.9595, 0.9730, and 0.9730, respectively. The AlexNet achieves 1.39%, 1.39%, 2.81%, 3.55%, and 4.29% improvement in accuracy compared to MobileNet-v2, ShuffleNet, GoogLeNet, SqueezeNet, and ResNet-50, respectively.

Table 3. The metric value comparison of deep learning models

Models	Accuracy	Precision	Sensitivity	Specificity	F1-score
ResNet-50	0.9459	0.9459	0.9459	0.9459	0.9459
SqueezeNet	0.9527	0.9351	0.9730	0.9324	0.9536
GoogLeNet	0.9595	0.9595	0.9595	0.9595	0.9595
ShuffleNet	0.9730	0.9605	0.9865	0.9595	0.9733
MobileNet-v2	0.9730	0.9861	0.9595	0.9865	0.9726
AlexNet	0.9865	0.9737	1.00	0.9730	0.9867

When deep learning models are compared in terms of error, the MobileNet-v2 achieves 0.9861 value. Those of AlexNet, ShuffleNet, GoogLeNet, SqueezeNet, and ResNet-50 are 0.9737, 0.9605, 0.9595, 0.9351, and 0.9459, respectively. Moreover, the MobileNet-v2 shows that the performance improvement of 1.27%, 2.66%, 2.77%, 5.45%, and 4.25% in precision than the AlexNet, ShuffleNet, GoogLeNet, SqueezeNet, and ResNet-50 respectively. Table 3 compares the sensitivity values of deep learning models. As can be seen, AlexNet outperforms other models with a value of 1.00. While ShuffleNet gives the best-second result with 0.9865, ResNet-50 has the worst value, which is 0.9459. The sensitivity values of SqueezeNet, GoogLeNet, and MobileNet-v2 are 0.9730, 0.9595, 0.9595, respectively.

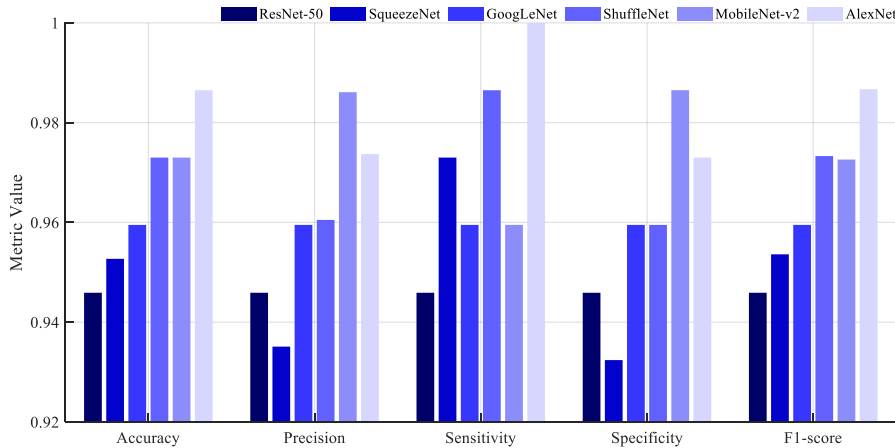


Figure 11. Comparison results of metric values for each deep learning models

When deep learning models are compared in terms of specificity values, when deep learning models are compared in terms of specificity values, MobileNet-v2 provides the best performance among all models. While AlexNet reaches the second-best result with a value of 0.9730, ResNet-50 shows the worst result with 0.9459. the MobileNet-v2 has an increase of approximately 1.39%–4.29% in terms of specificity compared to other models. When deep learning models are analyzed in terms of F1-score, AlexNet reaches the highest result with 0.9867. This result shows that the AlexNet is feasible. Those of MobileNet-v2, ShuffleNet, GoogLeNet, SqueezeNet, and ResNet-50 are calculated as being 0.9726, 0.9733, 0.9595, 0.9536, and 0.9459, respectively.

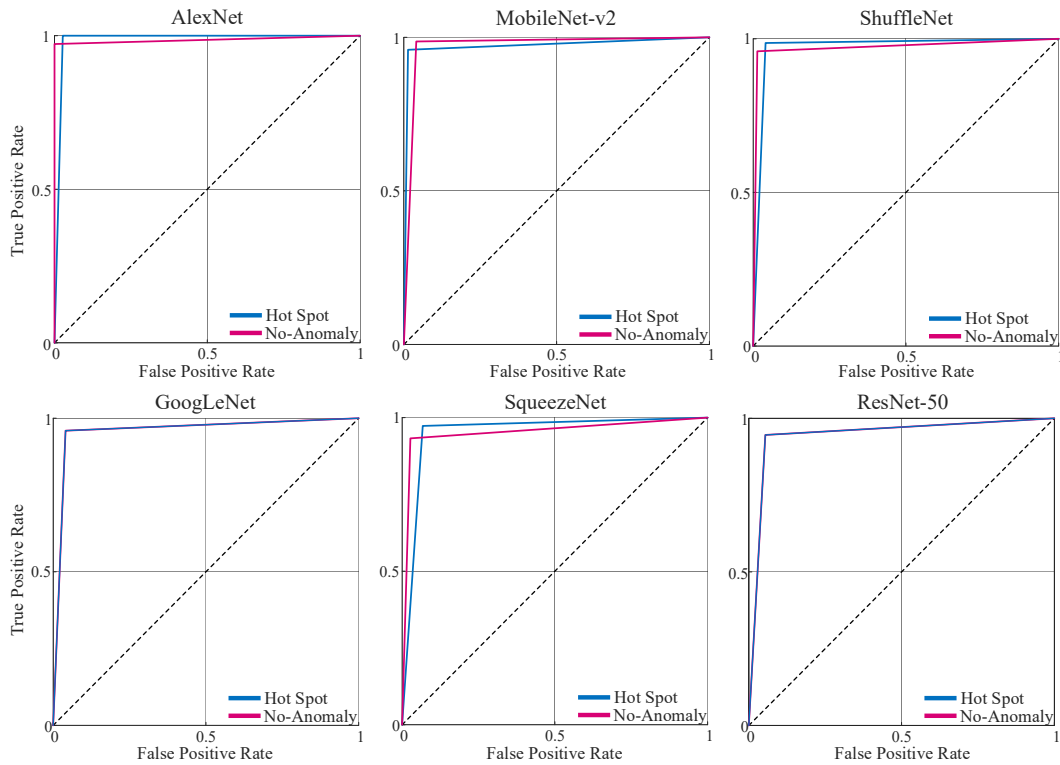


Figure 12. ROC curves of deep learning models

To get a better understanding and visualizing of the classification performances of deep learning models, Receiver Operating Characteristic (ROC) curves are given in Figure 12. As can be seen from Figure 11, AlexNet not only shows better classification ability, but also guarantees more effective results.

5. Conclusion

The fault-free operation of the PV modules directly affects the efficiency of the whole system. Although it is known that there are many fault classes in these modules, the most common fault class is the hotspot, which has an active role in the energy production of that module. For this reason, the detection and classification of hotspots in PV modules is considered as an important task. In recent years, deep learning, which is widely used in almost every sector and gives satisfactory results, has also taken its place in the solar energy sector. In this study, deep learning models namely AlexNet, MobileNet-v2, ShuffleNet, GoogLeNet, SqueezeNet, and ResNet-50 are used to classify hotspots in PV modules. All models are applied to the training dataset using the pre-trained model in the Matlab environment. The comparison studies are carried out by obtaining the values of performance evaluation metrics through experimental studies. AlexNet provides the highest accuracy, precision, and F1-score values, which are 0.9865, 1.00, and 0.9867, respectively. MobileNet-v2 reaches the highest precision and specificity values with 0.9861, and 0.9864, respectively. In future study, it is aimed to achieve better results by developing lightweight deep learning methods with different structures.

References

- [1] Korkmaz D, Acikgoz H, Yildiz C. A Novel Short-Term Photovoltaic Power Forecasting Approach based on Deep Convolutional Neural Network. *Int J Green Energy* 2021;1–15.
- [2] Korkmaz D, Acikgoz H. An efficient fault classification method in solar photovoltaic modules using transfer learning and multi-scale convolutional neural network. *Eng Appl Artif Intell* 2022;113:104959.
- [3] Korkmaz D. SolarNet: A hybrid reliable model based on convolutional neural network and variational mode decomposition for hourly photovoltaic power forecasting. *Appl Energy* 2021;300:117410.
- [4] Acikgoz H. A novel approach based on integration of convolutional neural networks and deep feature selection for short-

- term solar radiation forecasting. *Appl Energy* 2022;305:117912.
- [5] Wang Q, Paynabar K, Pacella M. Online automatic anomaly detection for photovoltaic systems using thermography imaging and low rank matrix decomposition. *J Qual Technol* 2021;0:1–14.
- [6] Ali MU, Khan HF, Masud M, Kallu KD, Zafar A. A machine learning framework to identify the hotspot in photovoltaic module using infrared thermography. *Sol Energy* 2020;208:643–51.
- [7] Ali MU, Saleem S, Masood H, Kallu KD, Masud M, Alvi MJ, et al. Early hotspot detection in photovoltaic modules using color image descriptors: An infrared thermography study. *Int J Energy Res* 2022;46:774–85.
- [8] Rahaman SA, Urmee T, Parlevliet DA. PV system defects identification using Remotely Piloted Aircraft (RPA) based infrared (IR) imaging: A review. *Sol Energy* 2020;206:579–95.
- [9] Cipriani G, D'Amico A, Guarino S, Manno D, Traverso M, Di Dio V. Convolutional neural network for dust and hotspot classification in PV modules. *Energies* 2020;13.
- [10] Dhimish M. Defining the best-fit machine learning classifier to early diagnose photovoltaic solar cells hot-spots. *Case Stud Therm Eng* 2021;25:100980.
- [11] Su B, Chen H, Liu K, Liu W. RCAG-Net: Residual Channelwise Attention Gate Network for Hot Spot Defect Detection of Photovoltaic Farms. *IEEE Trans Instrum Meas* 2021;70.
- [12] Manno D, Cipriani G, Ciulla G, Di Dio V, Guarino S, Lo Brano V. Deep learning strategies for automatic fault diagnosis in photovoltaic systems by thermographic images. *Energy Convers Manag* 2021;241:114315.
- [13] Kirsten Vidal de Oliveira A, Aghaei M, Rütther R. Aerial infrared thermography for low-cost and fast fault detection in utility-scale PV power plants. *Sol Energy* 2020;211:712–24.
- [14] Matthew M, Edward O, Vadhavkar N. Infrared Solar Module Dataset for Anomaly Detection. *Int Conf Learn Represent*. Published online 2020:1-5.
- [15] Krizhevsky, A, Sutskever, I, Hinton, GE. Imagenet classification with deep convolutional neural networks. In *Proceedings of the 25th International Conference on Neural Information Processing Systems*. 2012:1097-1105.
- [16] Zhang X, Zhou X, Lin M, Sun J. ShuffleNet: An extremely efficient convolutional neural network for mobile devices. *Proc. IEEE/CVF Conf. Comput. Vis. Pattern Recognit*. 2018:6848-6856.
- [17] Iandola FN, Han S, Moskewicz MW, Ashraf K, Dally WJ, Keutzer K. Squeezenet: Alexnet-level accuracy with 50x fewer parameters and <0.5 mb model size. *arXiv preprint arXiv:1602.07360*, 2016.
- [18] He, Kaiming, Xiangyu Zhang, Shaoqing Ren, and Jian Sun. Deep residual learning for image recognition. *Proc IEEE Comput Soc Conf Comput Vis Pattern Recognit*. 2016:770-778.
- [19] Szegedy C, Liu W, Jia Y, et al. Going deeper with convolutions. *Proc IEEE Comput Soc Conf Comput Vis Pattern Recognit*. 2015:1-9.
- [20] Sandler M, Howard A, Zhu M, Zhmoginov A, Chen LC. MobileNetV2: Inverted Residuals and Linear Bottlenecks. *Proc. IEEE/CVF Conf. Comput. Vis. Pattern Recognit*. 2018:4510-4520.